REAL-TIME MR IMAGING OF MYOCARDIAL REGIONAL FUNCTION WITH TISSUE THROUGH-PLANE MOTION TRACKING

E. H. IBRAHIM[1], R. ABRAHAM[1], A. S. FAHMY[1], M. STUBER[1], and N. F. OSMAN[1]
[1]JOHNS HOPKINS UNIVERSITY, Baltimore, MD, United States

INTRODUCTION

Strain-encoding (SENC) MRI provides direct imaging of myocardial strain through the acquisition of two images with different phase-encodings: low-tuning (LT) and high-tuning (HT) images (1). In addition, a technique has recently been proposed for real-time SENC imaging (2). However, the SENC technique, like other motion tracking techniques, suffers from the heart through-plane motion effects, which may adversely affect local strain computation. In this work, we propose a modification of the SENC technique for real-time myocardial strain imaging while tracking the original prescribed slice in the through-plane direction. This is accomplished by combining SENC and slice-following (3) techniques. We refer to the conventional SENC technique, the technique in (2), and the proposed technique as SENC, fast-SENC, and sf-fast-SENC, respectively.

METHODS and EXPERIMENTS

In slice-following, a thin slice is tagged (encoded) and then a thicker slab, that encompasses the tagged slice, is subsequently imaged. Three-dimensional spatially-selective magnetization preparation was implemented to reduce the FOV, thus reducing scan time, while enabling slice-following. After spatially-selective preparation of the magnetization, the area from which signal is obtained is confined to a thin disk. To cut the scan time into half in sf-fast-SENC, the two sets of LT and HT images are acquired in an interleaved way in a single breath-hold as described in (2). Spiral acquisition, with short spirals, is implemented to reduce scan time to a single heartbeat.

All experiments were performed on a 3T Philips scanner. The pulse-sequence is shown in Fig. 1. Because only one cardiac cycle is required for fast-SENC or sf-fast-SENC, the whole cardiac cycle could be imaged through end-diastole, which is not applicable in SENC. Two gel containers with cylindrical shapes were scanned while moving in and out of the imaging-plane. Ten healthy volunteers and five infarcted pigs were also scanned. The imaging parameters for sf-fast-SENC: 3 spirals×8 ms; TR/TE=11/1.2 ms; FOV=210×210 mm^2; diameter of the cylindrical excitation FOV=180 mm; scan matrix=64×256; encoding slice-thickness=10 mm; imaging slice-thickness=25 mm. For fast-SENC: imaging slice-thickness=8 mm; reduced excitation FOV=160×160 mm^2. For SENC: 12 spirals×12 ms; FOV=300×300 mm^2; TR/TE=20/1.2 ms. Standard grid-tagged SPAMM images were also acquired. The strain curves from the different SENC images were compared to those from the orthogonal SPAMM tagged images with and without tracking the tag intersection-points in the direction orthogonal to the SENC imaging-plane, which in SENC corresponds to applying and not applying slice-following, respectively. To examine the spatial resolution of sf-fast-SENC, delayed-enhancement (DE) images were acquired for the pigs. The bright (infarcted) regions in the DE image were compared to those in the sf-fast-SENC LT images, which show non-contracting myocardium.

RESULTS

Figure 2 shows the setup and results of the moving phantom experiment. One gel container totally disappeared after selective-excitation. The shape of the cross-section of the other container changed continuously (Fig. 2c, left to right) as the phantom moved forward and backward in the through-plane direction when imaging with fast-SENC. In contrast, the shape of the same phantom remained unchanged if sf-fast-SENC was used (Fig. 2d, left to right). Fig. 3 shows circumferential strain images from a volunteer experiment. The figure shows sf-fast-SENC and fast-SENC images of a long-axis slice. The figure also shows strain curves (Fig. 3c) computed for a ROI on the basal-septal LV wall. The resulting strain curves showed significant ($P<0.01$) difference between the strain values from sf-fast-SENC and fast-SENC images, especially at end-systole. In addition, there was similarity between the strain values from sf-fast-SENC and fast-SENC images and those from the corresponding SPAMM images with and without tracking the tag points, respectively (Fig. 3c). Fig. 4 shows results from the pig study. The figure shows a good agreement between the nonviable myocardium defined by hyperenhanced tissue in the DE image and the area of non-contracting (bright) myocardium in the sf-fast-SENC LT image.

CONCLUSIONS

A method is proposed for real-time black-blood myocardial functional imaging while considering the tissue through-plane motion. The resulting strain curves show differences from those obtained without slice-following. The method may support a fast and accurate quantification of local strain values.

REFERENCES

[1] NF Osman, *et al*, *Magn Reson Med*, 46:324-334.
[2] L Pan, *et al*, *Magn Reson Med*, 55:386-395.
[3] SE Fischer, *et al*, *Magn Reson Med*, 31:401-413.

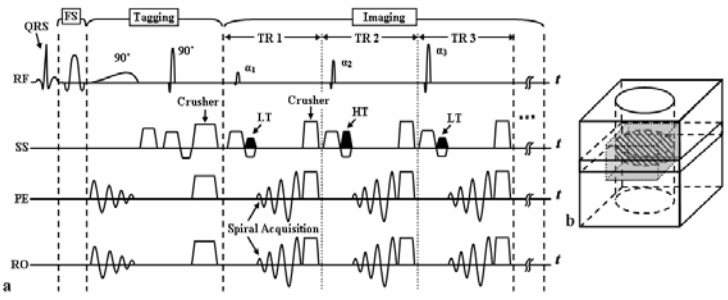

FIG. 1. (a) Pulse sequence diagram for sf-fast-SENC. (b) The tagged (dashed thin disk) and imaged (gray thick slab with reduced in-plane FOV) regions in sf-fast-SENC (FS = fat-suppression).

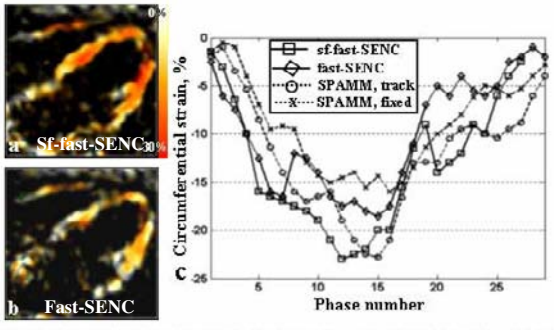

FIG. 3. Results of a volunteer experiment. (a) Sf-fast-SENC circumferential strain image. (b) Corresponding fast-SENC strain image. (c) Strain curves for a ROI on the basal-septal wall of LV.

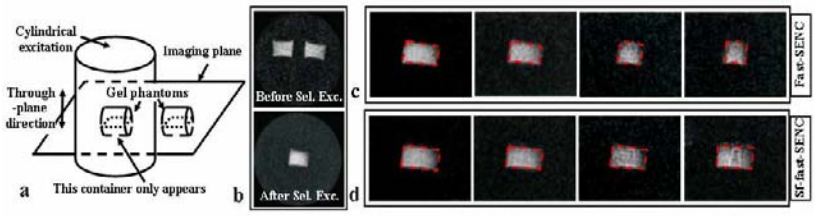

FIG. 2. (a) Setup of the moving phantom. (b) The effect of applying selective excitation. (c) A sequence of fast-SENC images during phantom motion (left to right). (d) A corresponding sequence of sf-fast-SENC images.

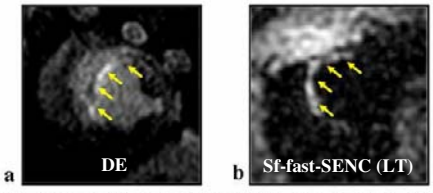

FIG. 4. Images from an infarcted pig at end-systole. (a) DE image showing infarction (arrows). (b) The corresponding sf-fast-SENC LT image showing non-contracting tissue (arrows).